Pergamon

0306-4522(94)00291-6

Neuroscience Vol. 63, No. 3, pp. 725–745, 1994
Elsevier Science Ltd

0306-4522/94 $7.00 + 0.00

CEREBELLAR-RESPONSIVE NEURONS IN THE THALAMIC VENTROANTERIOR–VENTROLATERAL COMPLEX OF RATS: LIGHT AND ELECTRON MICROSCOPY

S. F. SAWYER,* J. M. TEPPER†‡ and P. M. GROVES§

*Department of Physiology and Pharmacology, Bowman Gray School of Medicine, Wake Forest University, Medical Center Boulevard, Winston-Salem, NC 27157, U.S.A.
†Center for Molecular and Behavioral Neuroscience, Aidekman Research Center, Rutgers, The State University of New Jersey, 197 University Avenue, Newark, NJ 07102, U.S.A.
§Department of Psychiatry, School of Medicine, University of California at San Diego, La Jolla, CA 92093, U.S.A.

Abstract—The morphology and synaptic organization of neurons in the ventroanterior ventrolateral nucleus of rats was examined using *in vivo* intracellular staining techniques. Neurons were characterized electrophysiologically based on intrinsic membrane properties and synaptic responses to stimulation of motor cortex and cerebellar nuclei, as described in the companion paper. Cerebellar-responsive neurons were stained intracellularly with either horseradish peroxidase or biocytin. All stained ventroanterior–ventrolateral nucleus neurons were identified as thalamocortical neurons on anatomical (and often electrophysiological) grounds, consistent with previous findings that rat ventroanterior–ventrolateral nucleus is interneuron-sparse. Ventroanterior–ventrolateral nucleus neurons had three to eight thick primary dendrites. Proximal dendrites often exhibited a tufted branching pattern, from which many thinner, higher order dendrites arose. Dendrites branched to form a funnel-like infiltration of the neuropil that resulted in a spherical, roughly homogeneous dendritic field. The axon originated from the cell body or a proximal dendrite and coursed laterally and dorsally to innervate motor cortex. One to five axon collaterals were emitted in the rostral dorsolateral sector of the thalamic reticular nucleus; collaterals were not observed in the ventroanterior–ventrolateral nucleus or other nuclei in dorsal thalamus.

The synaptic organization of the ventroanterior–ventrolateral nucleus was examined with electron microscopy, including two intracellularly labeled ventroanterior–ventrolateral nucleus neurons that were shown electrophysiologically to receive monosynaptic inputs from the cerebellum. The neuropil of rat ventroanterior–ventrolateral nucleus lacked the complexity and diversity found in corresponding thalamic nuclei of felines and primates, due to the paucity of interneurons. Vesicle-containing dendrites, dendrodendritic synapses and glomeruli were not observed. Three broad classes of presynaptic terminals were identified. (1) Small round boutons: small boutons containing densely-packed, small round vesicles that formed asymmetric synapses predominantly with the distal dendrites of thalamocortical neurons. These were the most prevalent type of bouton in the ventroanterior–ventrolateral nucleus (78% of presynaptic elements) and likely arose from the cerebral cortex. (2) Large round boutons: large terminals with loosely packed small round vesicles that made multiple asymmetric synapses with proximal and intermediate dendrites. Large round boutons comprised 8% of the neuropil, and likely arose from the cerebellar nuclei. (3) Medium size boutons with pleomorphic vesicles: medium-sized profiles containing pleomorphic vesicles that formed symmetric synapses with proximal, intermediate and distal dendrites and, less frequently, with cell bodies. These boutons constituted 14% of the neuropil, and their morphology was similar to previous descriptions of GABAergic immunoreactive profiles in rat ventroanterior–ventrolateral nucleus, as well as boutons originating from the thalamic reticular nucleus (which is the primary source of GABAergic input to the ventroanterior–ventrolateral nucleus).

The synaptic organization of thalamocortical neurons and the scarcity of interneurons in the ventroanterior–ventrolateral nucleus is discussed in relation to the critical role of the thalamic reticular nucleus in modulating the efficacy of cortical and cerebellar afferents in the ventroanterior–ventrolateral nucleus and in determining the functional state of ventroanterior–ventrolateral nucleus neurons.

‡To whom correspondence should be addressed.

Abbreviations: dLGN, dorsal lateral geniculate nucleus; EPSP, excitatory postsynaptic potential; HRP, horseradish peroxidase; LR, large size boutons with round vesicles; MP, medium size boutons with pleomorphic vesicles; SR, small size boutons with round vesicles; TRN, thalamic reticular nucleus; VAL ventroanterior–ventrolateral.

The ventroanterior–ventrolateral (VAL) complex of rats receives excitatory afferents from the cerebellar nuclei and motor cortex.[4,13,25,36,93,118] Thalamic interneurons participate in triadic synaptic contacts with thalamocortical neurons, in which a subcortical afferent (e.g. from cerebellum) synapses onto dendrites of both thalamocortical neurons and interneurons, the latter forming a dendrodendritic synapse onto the dendrite of the relay neuron. Hence, interneurons provide an anatomical substrate for feedforward inhibition of thalamocortical neurons.[47,61]

However, unlike the corresponding motor-related thalamic nuclei in felines and primates, the VAL of rats contains few GABAergic interneurons.[91,115] The scarcity of interneurons in rat VAL raises a number of issues concerning the synaptic organization of thalamocortical neurons in this nucleus. Aside from the absence of inputs from interneurons, it remains to be clarified whether the density and spatial distribution of synaptic inputs onto thalamocortical projection neurons in rat VAL is comparable to that of projection neurons in feline and primate motor thalamus. The location of synaptic contacts along the dendritic expanse is an important determinant of the integrative properties of thalamic neurons, due to the heterogeneous distribution of ion channels along the somatodendritic membrane of thalamic neurons, many of which are voltage sensitive and therefore subject to influence from electrotonically adjacent synaptic inputs.[61,99,110] The focus of this investigation was to examine the morphology and synaptic organization of electrophysiologically-identified and intracellularly stained neurons in the VAL of rats whose electrophysiological properties are described in a companion paper.[93]

EXPERIMENTAL PROCEDURES

Intracellular staining and electrophysiological characterization

Methods used for *in vivo* intracellular recording, intracellular staining, electrophysiological characterization of neurons and intracranial electrical stimulation are presented in the companion paper.[93] Briefly, following impalement of a VAL neuron with a glass micropipette containing horseradish peroxidase (HRP) or biocytin, the ipsilateral motor cortex and contralateral cerebellar nuclei were stimulated to evoke antidromic (from cortex) and synaptic responses. Following electrophysiological characterization, neurons exhibiting monosynaptic excitatory postsynaptic potentials (EPSPs) from cerebellar stimulation were injected with HRP or biocytin. Only one neuron was stained per animal.

Tissue processing

One to three hours after injection of intracellular label, the animals were given heparin (4000 units/kg, i.p.) and a lethal dose of urethane. While deeply anesthetized, animals were then perfused intracardially with 50–100 ml of oxygenated Ringer's (pH 7.2) followed with 300 ml of 1% paraformaldehyde and 2% glutaraldehyde in Sörensen's phosphate buffer (pH 7.2, 0.15 M). Brains were removed, blocked and stored in buffer at 4°C. One to three days later, 60–70 μm coronal sections were cut with a Vibratome and washed in cold buffer. For HRP injections, the tissue was processed for the histochemical detection of HRP with the glucose oxidase method of Itoh *et al.*[44] using 3,3′-diaminobenzidine as the chromogen. One HRP-filled neuron (Fig. 3A) was processed for light microscopic analysis only; all other HRP-injected neurons were processed for sequential light and electron microscopy. Sections were washed in buffer, postfixed in 0.5% osmium tetroxide for 45–60 min, dehydrated in an ascending series of ethanol, stained *en bloc* with 1% uranyl acetate in 70% ethanol, cleared in an ascending series of acetone, infiltrated and embedded in Spurr's medium and placed between Teflon-coated coverslips and slides, then cured for 54–72 h at 60–70°C.[116] Tissue processed for the detection of biocytin-filled neurons[40] was sectioned and washed in 0.1% glycine in phosphate buffer, 0.5% hydrogen peroxide in buffer, and then buffer alone. Sections were incubated for 4 h at room temperature in 0.5% Triton X-100 that contained avidin–biotin complex (1:200 dilution; Vector Labs) in phosphate buffer, and then washed and placed in 0.05% 3,3′-diaminobenzidine and 0.01% H_2O_2 in buffer for 20 min. Following osmication for 10 min in 0.1% OsO_4, sections were washed in buffer, mounted on slides and dehydrated. Cortical stimulating sites were confirmed from inspection of thalamic sections. Cerebellar stimulating sites were determined from frozen sections stained with Neutral Red.

Light and electron microscopic analysis

Tissue sections were examined with a Leitz OrthoLux II light microscope using ×50 and ×100 oil immersion objective lenses. Camera lucida drawings of intracellularly-injected neurons were accomplished with a drawing tube attachment.

Two neurons (T56.2 and T116.2) in the VAL that were intracellularly stained with HRP were selected for further examination with electron microscopy. After complete light microscopic analysis, sections containing these labeled cell bodies and processes were stripped free of the Teflon-coated coverslips and slides, and areas of interest trimmed out and mounted onto epoxy blocks. Thin sections (70–100 nm) were cut on an ultramicrotome, positioned on mesh or Formvar-coated slot grids, and poststained with 4% uranyl acetate in methanol for 20 s and 0.3% lead citrate for 3–5 min. Ultrastructure was examined with JEOL 100CX or 100B electron microscopes.

Morphometrics and statistics

The cross-sectional surface area of cell bodies (camera lucida drawings) and presynaptic terminals (electron micrographs) were determined by tracing the outline of these profiles onto a Summagraphics digitizing tablet and calculating the area within the outline with a morphometric computer program.[122] The diameter of postsynaptic profiles was assessed from the site of synaptic contact. Statistical analyses of morphometric data utilized the Kolmogorov–Smirnov two-sample cumulative distribution function test and the Tukey HSD test. Data are presented in the text as mean ± S.E.M.

RESULTS

Light microscopy of intracellularly labeled neurons

Electrophysiological identification and anatomical localization. A total of 16 cerebellar responsive neurons were labeled intracellularly with HRP or biocytin and recovered in a form suitable for further analysis. Thirteen of the recovered neurons were located in the VAL, and all of these responded to cerebellar stimulation with a monosynaptic EPSP (2.48 ± 0.26 ms onset latency) Seven of the 13 stained VAL neurons were also antidromically activated from ipsilateral motor cortex. Two cerebellar-responding neurons

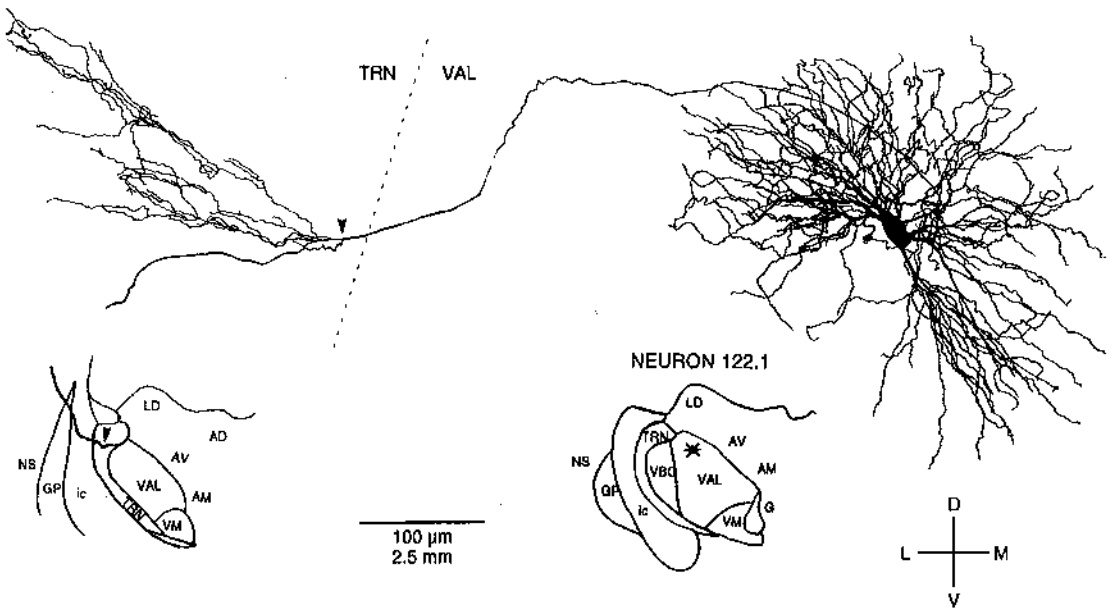

Fig. 1. Camera lucida drawing of a biocytin-stained Type 1 cerebellar-responsive thalamocortical VAL neuron. The axon of this projection neuron coursed rostrolaterally to enter the TRN. A single collateral was emitted within the TRN (arrowhead) which gave rise to a dense collateral field. Note the absence of axon collaterals within the VAL. Bottom left shows a low magnification perspective of the route taken by the main axon (arrowhead) through the TRN and the internal capsule. At more rostral levels, the axon was traced into motor cortex (not shown). Dashed lines indicate boundaries of VAL and TRN. The scale bar pertains to both higher and lower magnification drawings.

were located in the ventrobasal complex, and exhibited EPSPs wtih variable onset latencies (3–3.5 and 10–11 ms, respectively). The remaining neuron was located in the posterior nucleus and responded to cerebellar stimulation with a monosynaptic EPSP (2.05 ms latency).

Somatodendritic morphology of cerebellar-responsive ventroanterior–ventrolateral neurons. A previous Golgi study of the VAL in rats identified four morphologically distinct types of neurons,[92] and we classified intracellularly stained VAL neurons with respect to this scheme. Labeled VAL neurons were categorized as either Type 1 (12 neurons) or Type 3 (one neuron). Camera lucida drawings and photomicrographs of selected Type 1 neurons are illustrated in Figs 1–3 and 4A. These neurons had medium- to large-sized cell bodies ($26 \pm 2 \times 17 \pm 1\ \mu m$; $327 \pm 11\ \mu m^2$) and three to eight thick proximal dendrites that branched to form thinner dendrites. Usually, at least one dendrite exhibited a complex and dense branching pattern in which four or more thin branches arose from a thick dendritic stump (Fig. 2), a pattern that has previously been termed a "tuft"[95] or "whorl".[60] Tufted branching often consisted of a collection of radially-oriented secondary dendrites that spiraled about an axis perpendicular to the cell body, reminiscent of a funnel.[92] Branching of tertiary and higher order dendrites usually consisted of bifurcations. The overall form of the dendritic field was spherical with a diameter of 300–400 μm, but dendritic field density was often somewhat heterogeneous due to tufting. The Type 3 neuron (Figs 4B, 5) was located in the dorsolateral subdivision of the VAL and had a medium-sized cell body ($25 \times 14\ \mu m$; $260\ \mu m^2$), stout primary dendrites, and a large and spherical dendritic field with a diameter of 450–500 μm.

Intracellularly stained VAL neurons had spine-like appendages that covered the surface of dendrites distal to the first branch point (0.5–1.5 spines per μm dendritic length) but were scarce on the cell body and primary dendrites (Figs 2, 5). Spinous appendages exhibited a variety of shapes, the most common being squat sessile blebs (found along the entire length of the dendrites). Other types of dendritic appendages

Fig. 2 (*overleaf*). High magnification photomontage of a portion of the neuron shown in Fig. 1. The soma and proximal dendrites were spine-free. More distal dendritic segments were covered with a variety of spinous extrusions, ranging in form from squat blebs to long, slender stalks (small arrowheads). The thick proximal dendrites branched into numerous thinner, radiating dendrites. The asterisk labels a proximal dendrite with a tufted branching pattern, from which numerous thinner dendrites arose from a single branch point. The axon is indicated with the larger arrowhead. The white dot labels an erythrocyte. Dorsal is up, lateral is left.

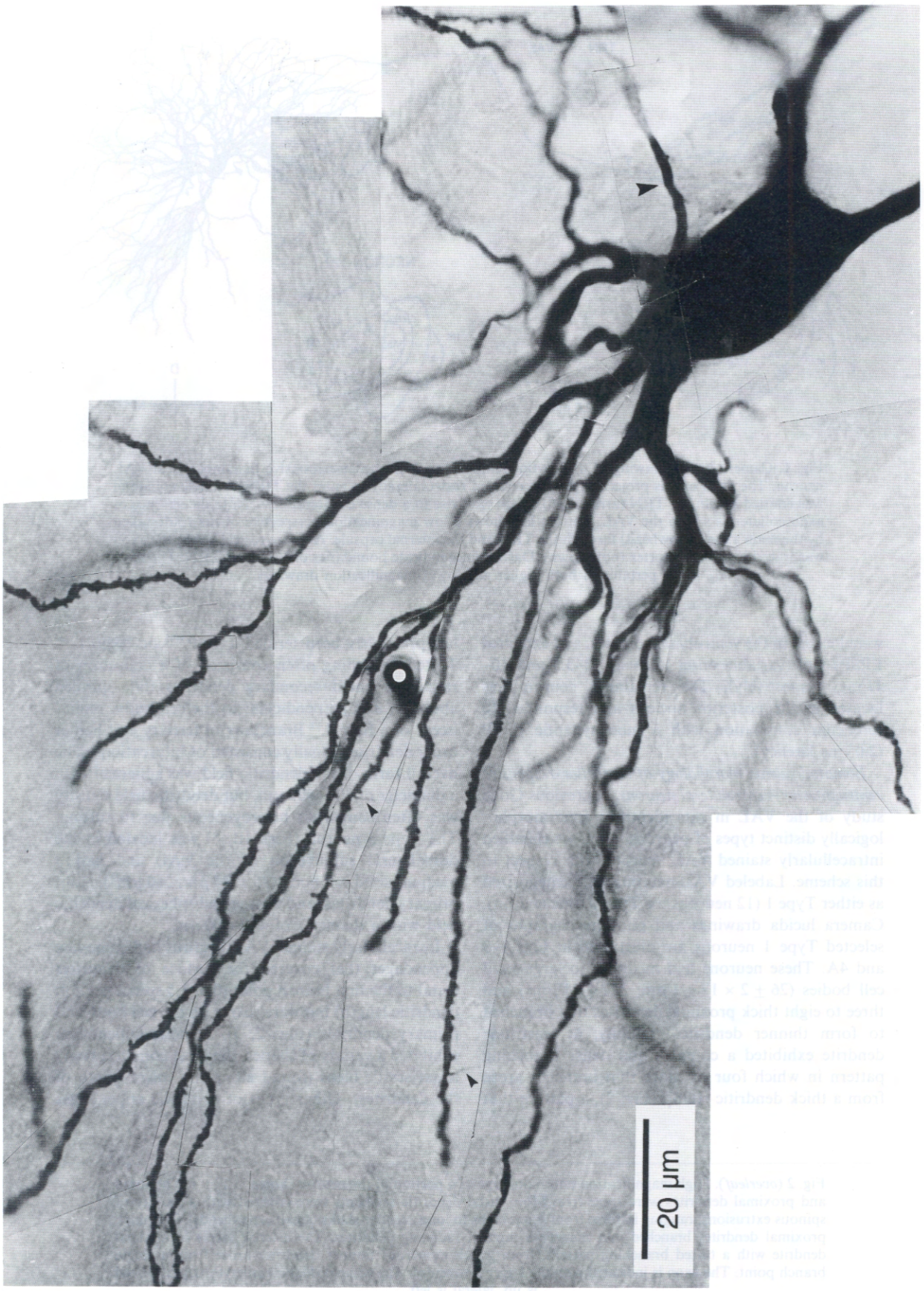

Fig. 2—*legend on p. 727.*

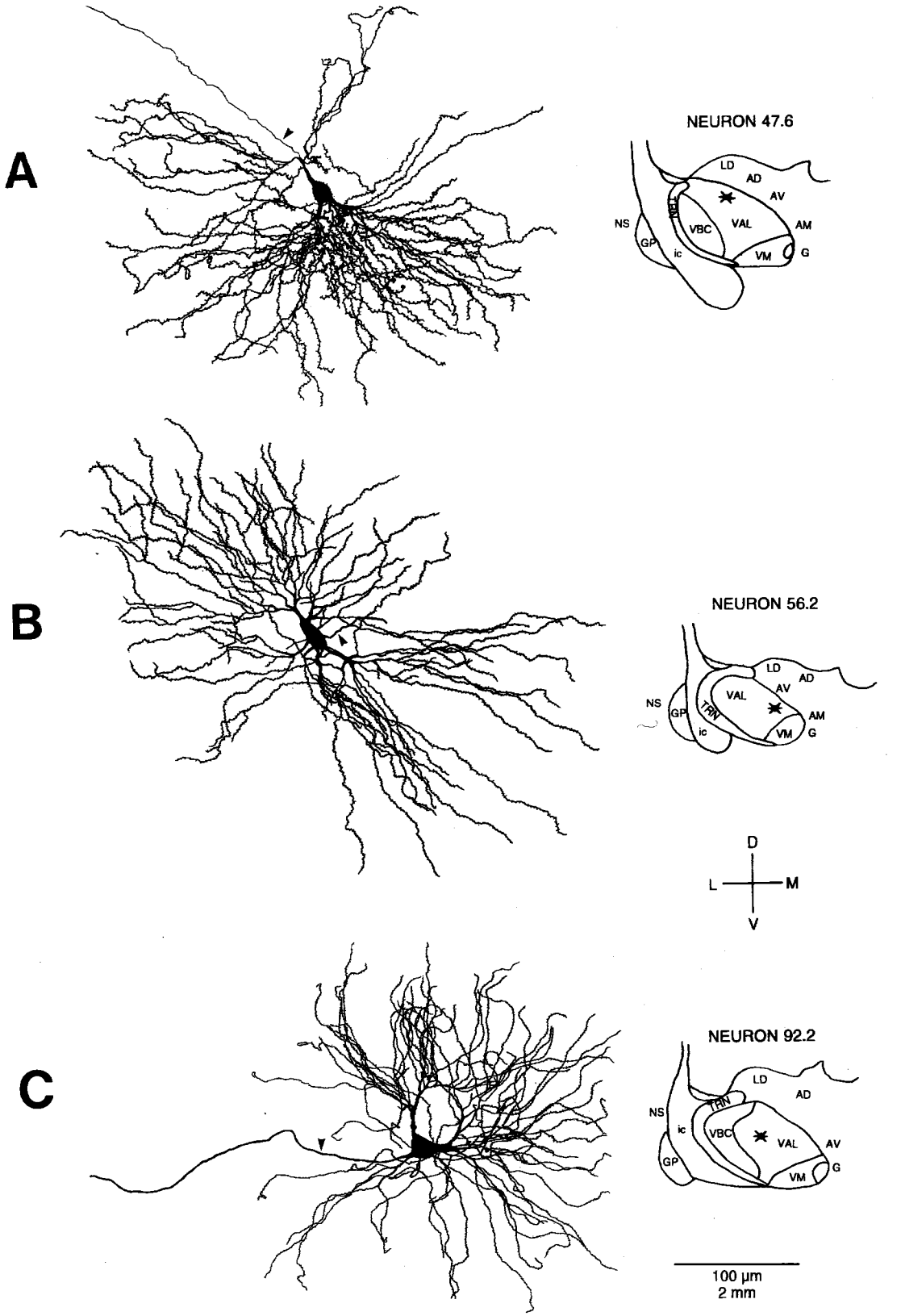

Fig. 3. Camera lucida drawings of somatodendritic morphology of three HRP-labeled, cerebellar-responsive thalamocortical Type 1 neurons in the VAL. Low magnification drawings provide a perspective for location of the cell bodies. As was characteristic of Type 1 neurons, the soma gave rise to thick primary dendrites from which thinner, radially-directed branches emanated. Arrowheads point to axons, which were traced into motor cortex. Axon collaterals of neurons in A and C are illustrated in Fig. 6.

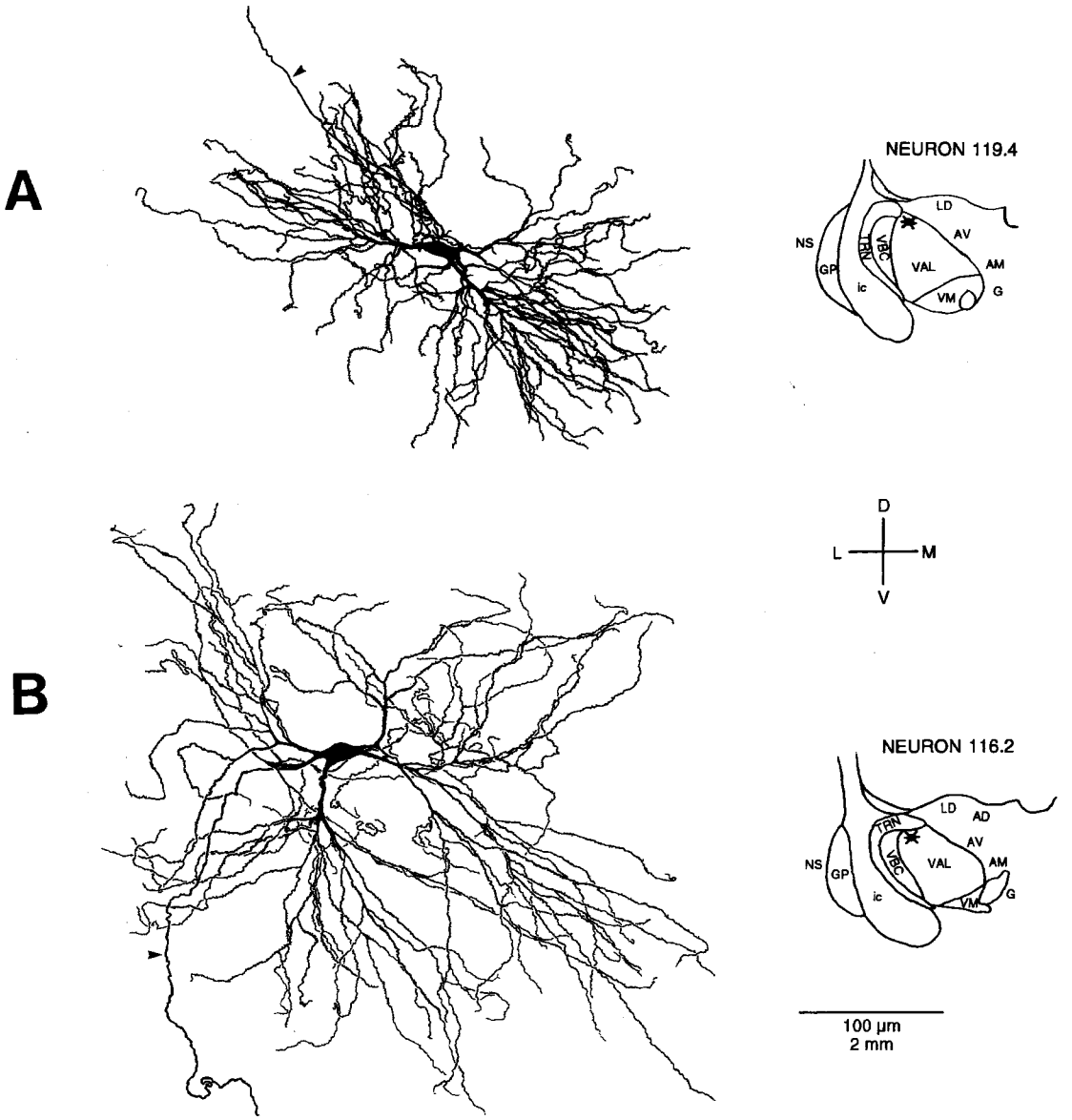

Fig. 4. Camera lucida drawings of intracellularly stained cerebellar-responsive Type 1 (A) and Type 3 (B) thalamocortical neurons in VAL. The intracellularly labeled Type 3 neuron was characterized by the large expanse of its dendritic field and a location restricted to dorsolateral VAL. The illustrated Type 1 neuron was also located in the dorsolateral VAL, but had a smaller and denser dendritic field than the Type 3 neuron. Axons (arrowheads) of both neurons were traced into motor cortex.

consisted of long thin stalks (located distally) and large bulbous protuberances (situated proximally, usually at branch points).

Axon collaterals in the thalamic reticular nucleus. All intracellularly stained VAL neurons had a single axon that emerged from either the soma or a proximal dendrite. Within a short distance, the axon entered one of the many fiber bundles that penetrate the VAL and traveled laterally towards the thalamic reticular nucleus (TRN). Local axon collaterals were not observed within the VAL or any other dorsal thalamic nucleus. Labeled axons entered the TRN perpendicular to the TRN–dorsal thalamus border, and emitted one to five thin collaterals at right angles to the main axon. These collaterals remained entirely within the TRN, parallel to the borders of this nucleus (although this anatomical attribute is not always evident from the two-dimensional renderings presented in Figs 1 and 6). Individual collaterals occupied a restricted sector of the TRN, usually less than one-fifth the width of the nucleus, although cumulatively the collaterals from an axon could innervate two or three parallel sectors in the TRN (Fig. 6B, C).

Three types of axon collaterals were recognized in the TRN: (i) non-varicose, short (less than 125 μm) and sparsely branched collaterals that had a restricted

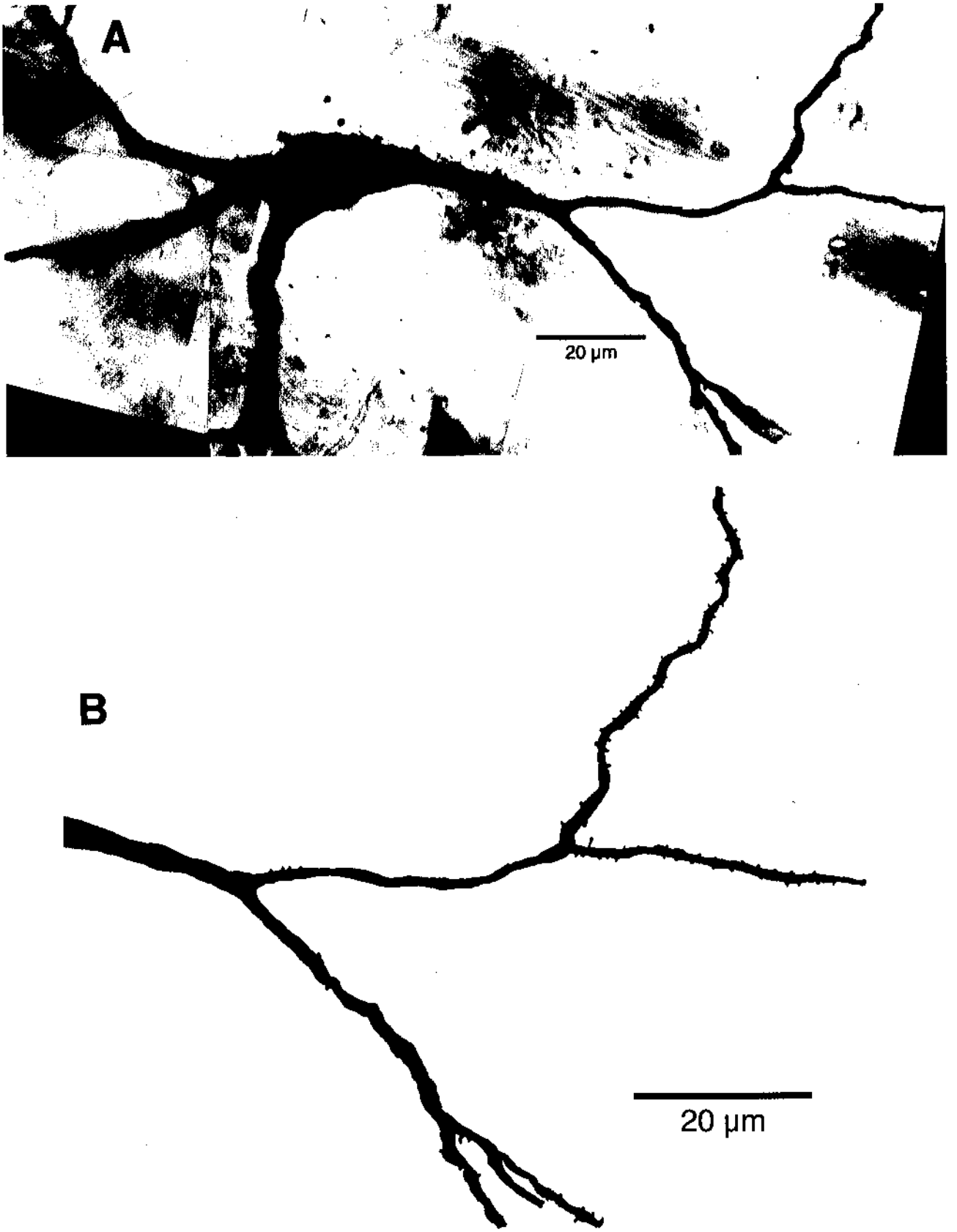

Fig. 5. Light micrographs (A) and camera lucida drawing (B) of the Type 3 neuron illustrated in Fig. 4B. Spinous extrusions were prevalent on secondary and higher order dendrites. Drawing in B corresponds to the dendrites in the right half of A. Dorsal is up, lateral is to left.

field (leftmost collateral in Fig. 6A, D); (ii) longer collaterals with numerous varicosities that were extensively branched and encompassed a cylindrical field (100–350 μm by 50–100 μm; Fig. 1; the right and central collaterals in Fig. 6A; right collateral in Figs 6C, 7B); and (iii) long (up to 300 μm) and unbranched varicose collaterals that followed the contour of the TRN, and whose position along the rostrocaudal axis was essentially unchanged, e.g. these long collaterals were usually confined to a single 70 μm coronal section (leftmost collaterals in Fig. 6C). Varicosities were present along the entire length of the varicose collaterals, but were more common near the termini. The distance between varicosities ranged from 5 to 20 μm. The diameter of the main axon was typically about 1.5 μm, whereas the collaterals were 0.2–0.4 and 1.0–1.5 μm thick in non-varicose and varicose segments, respectively. Electron microscopy confirmed that the main axon was myelinated and the collaterals were not (data not shown). All three types of axon collaterals were observed to arise from Type 1 neurons, but all variants were not necessarily evident from the same axon. The Type 3 neuron had both types of varicose collaterals. After exiting the TRN laterally, the axons entered the internal capsule and coursed rostrodorsally towards the cerebral cortex, sometimes passing through the striatum. Axons were traced as far as layer VI of motor cortex.

Fine structure and synaptic organization of the ventroanterior–ventrolateral complex

Since the electron-dense HRP reaction product often obscured the ultrastructural cytological details of the labeled neurons, the fine structure of unlabeled VAL tissue will be briefly discussed and related to the synaptic organization of the injected neurons. Cell bodies of neurons in the VAL were ovoid or elongated, 20–35 μm in diameter in the long axis. The centrally located pale nucleus typically had an indented membrane and a dark nucleolus. The perikarya had a granular appearance due to an abundance of free ribosomes and Nissl substance. The cytoplasmic constituents of perikarya extended into the base of dendrites. The cytoplasm of more distal dendrites possessed neurofilaments, oval and elongated mitochondria, longitudinally oriented microtubules and smooth endoplasmic reticulum. Dendritic extrusions, corresponding to the squat blebs observed at the light microscopic level, were present on small- and medium-diameter dendrites and were a common target for synapses. Dendritic extrusions were not associated with any specialized cytoplasmic organelle, such as a spine apparatus, although the cytoplasm within extrusions was more flocculent than in the dendrite.

Three broad classes of boutons were distinguished in the VAL at the ultrastructural level.

Small round bouton profiles. The most common profile in the neuropil (78% of the total), these small (cross-sectional surface area = 0.25 ± 0.01 μm^2; $N = 174$) spherical boutons with round vesicles (SR; 40–60 nm diameter) formed a long and prominent asymmetric synaptic contact, usually with small diameter dendrites and often on dendritic extrusions (Fig. 9). Vesicles were present in relatively high density (246 ± 11 vesicles per μm^2; $N = 69$ boutons) and tended to cluster near the active zone. Mitochondria were rarely observed in these boutons, but were present in the thin unmyelinated preterminal axons from which SR boutons arose.

Large round bouton profiles. These boutons were distinctive for their large size (cross-sectional surface area = 1.66 ± 0.32 μm^2; $N = 18$) (Fig. 9E). Vesicles were round and slightly smaller (LR; 30–45 nm) than those in SR boutons, and filled the bouton in a somewhat clumpy fashion, with a density of 139 ± 13 vesicles per μm^2 ($N = 14$ boutons). LR boutons had numerous centrally positioned mitochondria that were surrounded by neurofilaments. LR boutons made multiple asymmetric synaptic contacts onto medium to large diameter dendrites, although the postsynaptic density was less prominent than for synapses formed by SR boutons. LR boutons were often observed to synapse on more than one dendrite in a single thin section, and sometimes completely engulfed thinner dendrites; the boutons themselves were usually surrounded by a thin glial sheath. LR boutons also formed numerous puncta adhaerentia. LR boutons constituted 8% of the terminals observed in the VAL (although it is worth noting that the single section analysis used in this study would be expected to overestimate the proportion of LR boutons owing to the large size of these profiles).

Medium size pleomorphic bouton profiles. These boutons were medium sized (cross-sectional surface area = 0.71 ± 0.13 μm^2; $N = 40$), contained a mix of pleomorphic vesicles (MP; flat, elliptical or round; 35–55 nm × 25–45 nm) and had a variable number

Fig. 6. Camera lucida drawings of axon collaterals emitted within the TRN by cerebellar-responsive thalamocortical VAL neurons. Somatodendritic morphology of these neurons is illustrated in Figs 3 and 4. Collaterals of Type 1 (A, B, D) and Type 3 (C) neurons. Arrowheads indicate origin of collaterals. The extent of collateralization varied: some collaterals had few branch points and relatively non-varicose processes (B, D, left collaterals in A and C), whereas other processes extensively infiltrated the TRN with numerous varicose branches (rightmost collaterals in A and C). The fields of individual collaterals penetrated a relatively small cylindrical volume of the TRN, and the plane of arborization was generally parallel to the borders of the TRN. Boxed areas in A are shown in Fig. 7. Dashed lines indicate boundaries of the TRN.

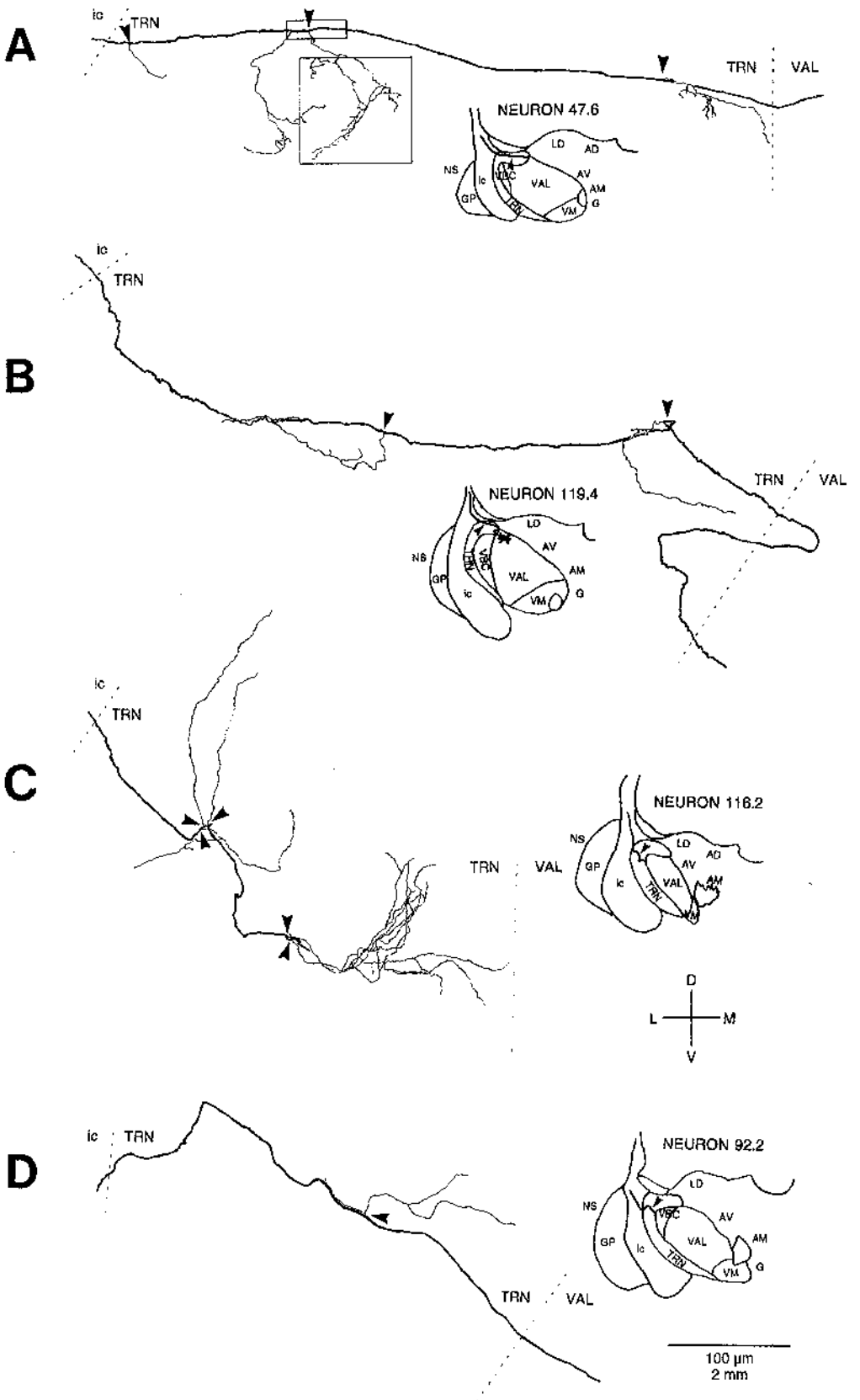
A
ic
TRN
TRN
VAL
NEURON 47.6
LD
AD
NS
ic
VSC
AV
VAL
AM
GP
TRN
VM
G
B
ic
TRN
TRN
VAL
NEURON 119.4
LD
AV
NS
VSC
GP
AM
VAL
ic
VM
G
C
ic
TRN
TRN
VAL
NEURON 116.2
NS
LD
AD
GP
AV
ic
VAL
AM
TRN
VM
D
L
M
V
D
ic
TRN
NEURON 92.2
TRN
VAL
LD
NS
VSC
AV
GP
VAL
AM
ic
TRN
VM
G
100 µm
2 mm

Fig. 6.

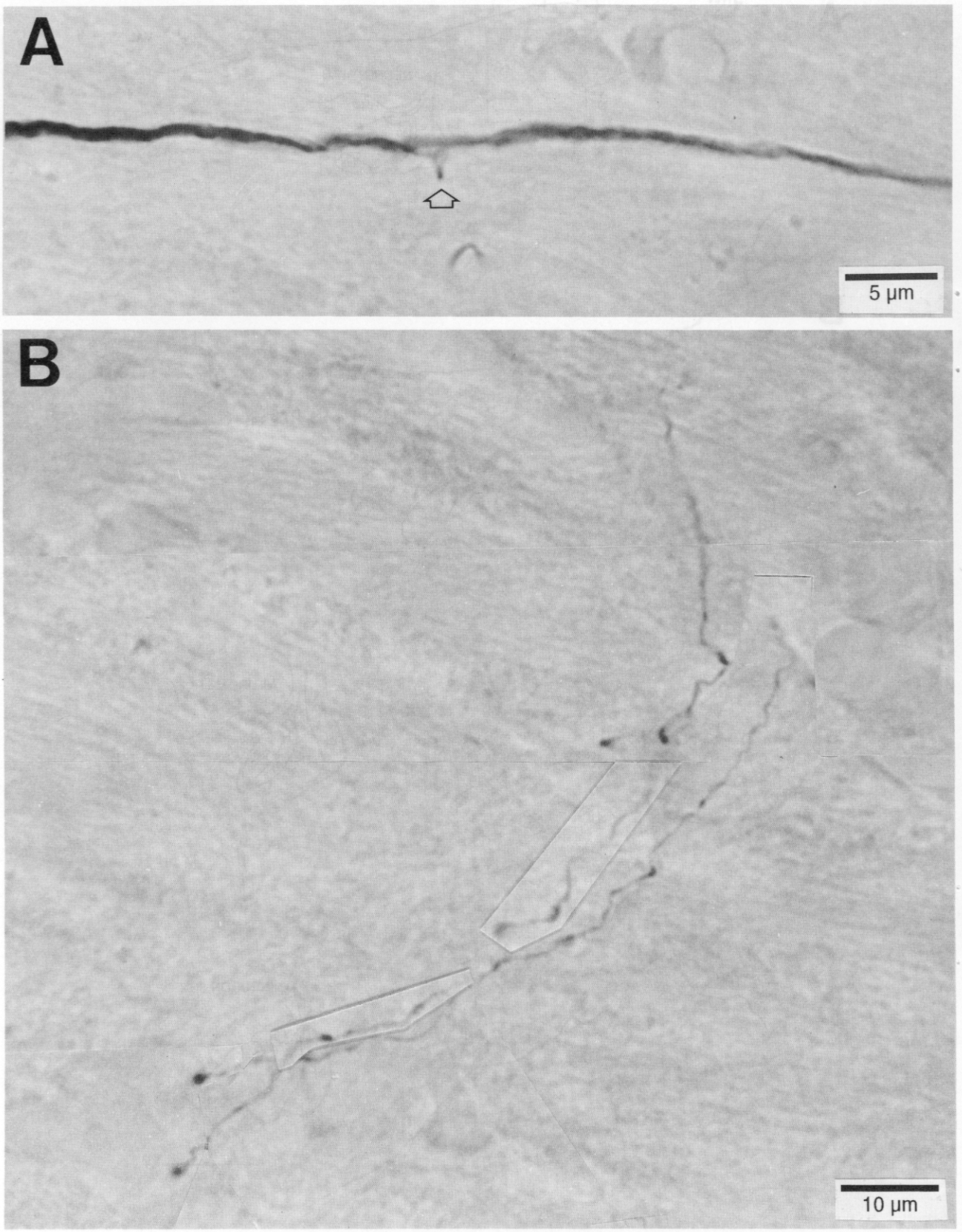

Fig. 7.

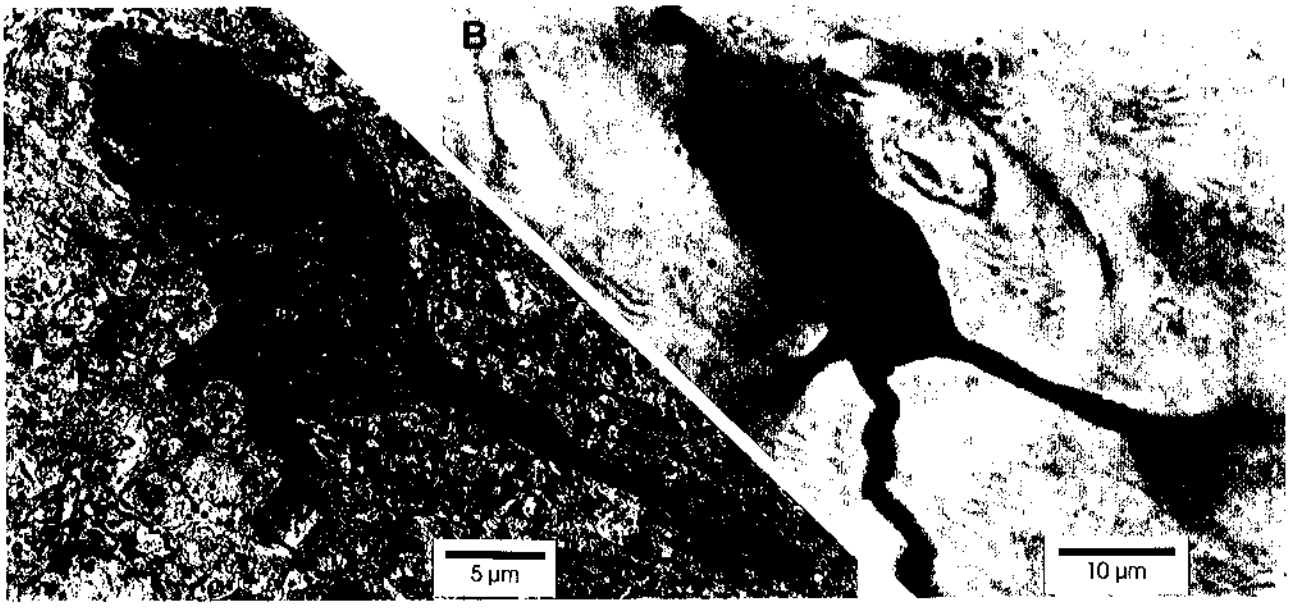

Fig. 8. Low magnification electron micrograph (A) and light micrograph (B) of intracellularly labeled cerebellar-responsive Type 1 neuron. The somatodendritic morphology of this neuron is illustrated in Fig. 3B. The soma (S) is heavily stained with electron-dense HRP reaction product. There were no synapses on the soma in this section.

usually onto medium to large diameter dendrites, but also onto distal dendrites and cell bodies (Fig. 9A). Vesicles were often uniformly dispersed throughout the bouton, although MP boutons exhibited a wider range of vesicle density (211 ± 29 vesicles per μm^2; $N = 20$ boutons) than LR or SR boutons. Puncta adhaerentia were observed, but not with the abundance found with LR boutons. The MP boutons described in this report were morphologically identical to MP boutons found to be GABA-immunoreactive in a previous study of rat VAL ultrastructure.[91] MP boutons accounted for 14% of the observed terminals in the VAL.

There was a statistically significant difference between the cross-sectional surface area of the three classes of boutons for all pairwise comparisons, with SR boutons being smallest and LR boutons largest (Tukey HSD; $P < 0.001$ for all comparisons). Vesicle density was greater in SR boutons than in LR boutons (Tukey HSD; $P < 0.001$), whereas vesicle density in MP boutons was not significantly different from that of LR or SR boutons (Tukey HSD; $P > 0.05$). The distributions of these two parameters for the three bouton types are illustrated in Fig. 10.

Glomeruli and presynaptic dendrites. Glomeruli were not observed in the VAL. However, one characteristic of glomeruli was occasionally observed in the VAL, namely an LR bouton in synaptic contact with one or more dendrites that were spatially-segregated from the surrounding neuropil by electron-pellucid astrocytic processes. In contrast to these non-glomerular "synaptic islands", the remaining neuropil consisted of either densely packed boutons (mostly of SR type) and dendrites (Fig. 9B) or a more dispersed arrangement that included postsynaptic targets and all three bouton types. Characteristic features of dendrites of thalamic interneurons, such as vesicle-containing postsynaptic elements and dendrodendritic synapses, were not observed in the VAL. In addition, no presynaptic profiles were labeled with HRP, consistent with the absence of presynaptic dendrites in VAL as well as light microscopic determination that the two intracellularly stained neurons did not issue local axon collaterals in dorsal thalamus.

Synaptic organization of intracellularly labeled neurons

Two intracellularly labeled neurons located in the VAL that were monosynaptically activated by cerebellar stimulation were subjected to electron microscopic analysis. One of the neurons was categorized as Type 1 (T56.2; Figs 3B, 8) and the other as Type 3 (T116.2; Figs 4B, 5). A low magnification electron micrograph of the soma and a proximal dendrite of the Type 1 neuron is shown in Fig. 8A. As was

Fig. 7. Photomontages of an axon collateral in the TRN, from the HRP-labeled VAL neuron depicted in Figs 3A and 6A (and Fig. 1 of companion paper[93]). (A) Origin of collateral as it emerged from the main axon (arrow), corresponding to smaller box in Fig. 6A. Remainder of collateral segment was located in adjacent tissue sections. (B) Photomontage of area depicted in larger box of Fig. 6A. Collaterals were varicose along their length, especially distally.

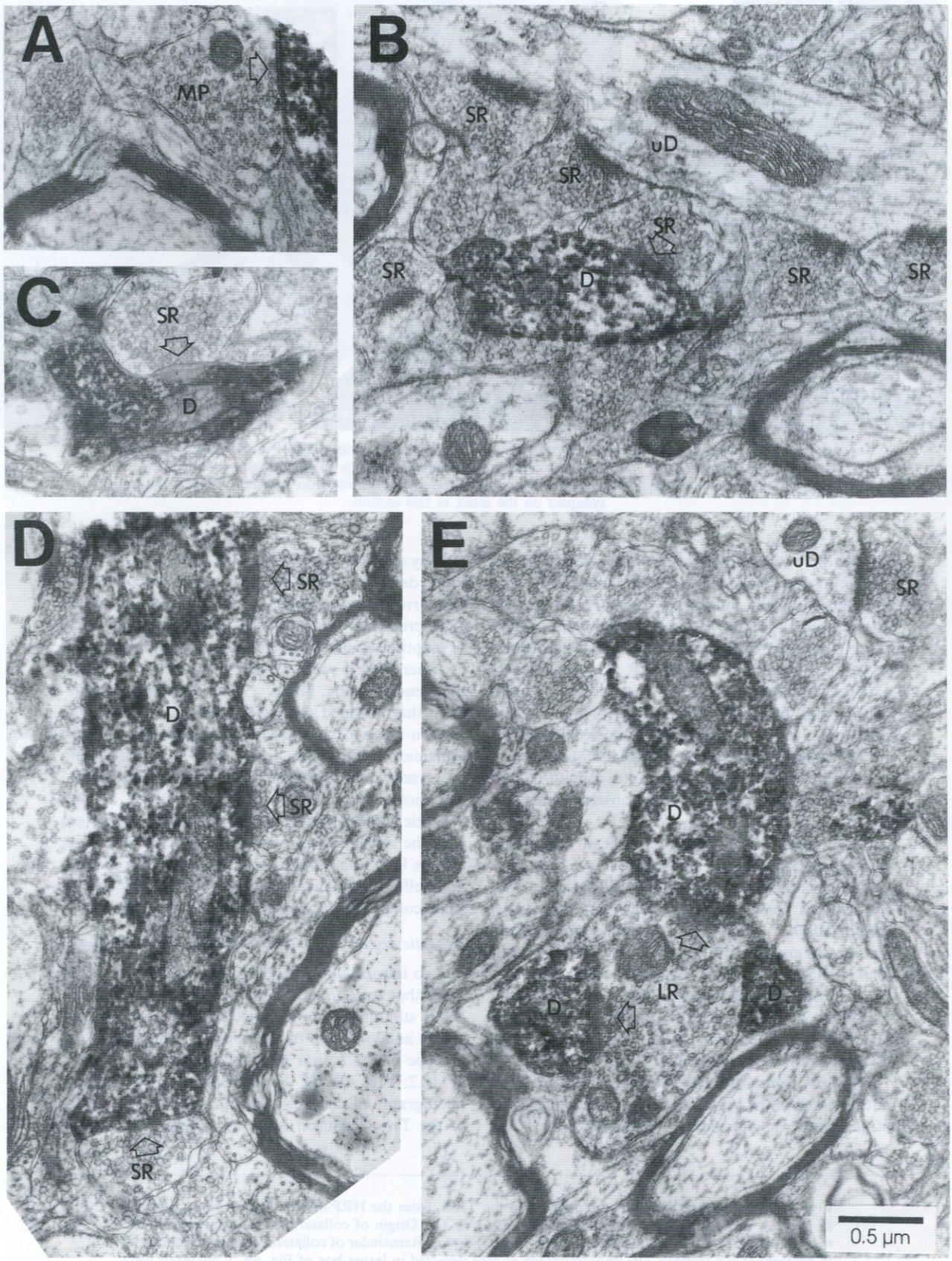

Fig. 9.

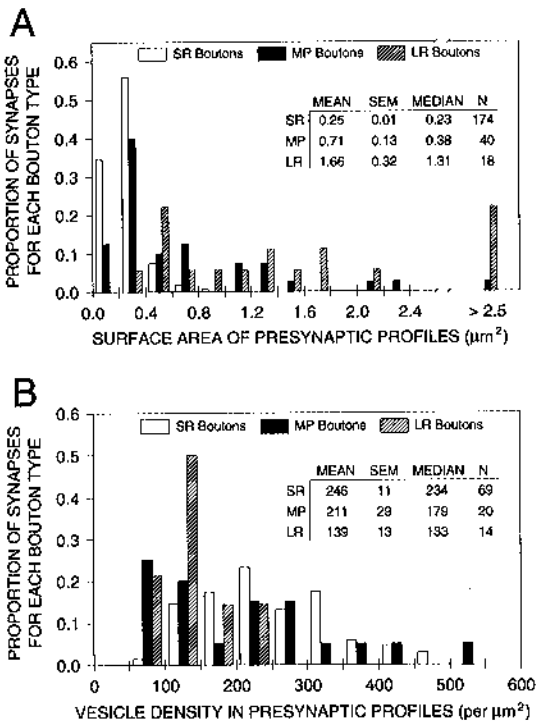

Fig. 10. Graphical summary of morphometrics for synaptic boutons in rat VAL. Histograms of the cross-sectional surface area (A) and bouton vesicle density (B) for the three types of boutons. The surface areas of all three boutons were statistically significantly different from each other (Tukey HSD; $P < 0.001$ for all comparisons). Vesicle density was greater in SR boutons than in LR boutons (Tukey HSD; $P < 0.01$), but MP boutons did not differ from the other bouton types. Data are presented as the proportion of synapses for each bouton type.

characteristic of neurons in the VAL, few synapses were found on the soma. Likewise, proximal dendrites had a lower density of synaptic contacts than intermediate and distal dendrites. The synaptic organization of the Type 3 cell was examined more extensively, and the following discussion pertains to that neuron, although the findings are also applicable to the Type 1 neuron.

The three classes of boutons described above formed synaptic contacts with the HRP-labeled Type 3 neuron. SR boutons terminated predominantly on intermediate (25–125 μm from soma) and distal (> 125 μm from soma) dendrites (110 $\pm$ 6 μm from soma; median = 122 μm; $N = 68$). LR boutons synapsed onto proximal (< 25 μm) and intermediate dendrites (64 $\pm$ 11 μm; median = 75 μm; $N = 8$), whereas MP boutons were distributed along all regions of the neuron (84 $\pm$ 18 μm; median = 75 μm; $N = 8$). The spatial distribution of synaptic inputs onto the Type 3 neuron (T116.2) is shown graphically and schematically in Fig. 11C, D. The distribution of LR boutons was statistically different from that of SR boutons (Kolmogorov–Smirnov test; $P < 0.05$), whereas the distribution of MP boutons, being more variable, was not statistically different from either SR and LR boutons. The proportion of each type of presynaptic bouton was similar to that observed for unlabeled postsynaptic targets: SR boutons were most common, constituting 78% of the observed presynaptic elements that synapsed onto the neuron, whereas MP boutons contributed 13% of presynaptic profiles and LR boutons the remaining 9%. The synaptic organization of this intracellularly injected neuron was similar to that of the unlabeled

Fig. 9. Electron micrographs of synaptic contacts onto proximal and intermediate dendritic regions of the HRP-labeled Type 3 (A, B, D, E) and Type 1 (C) neurons shown in Figs 4B and 3B, respectively. (A) MP bouton with pleomorphic vesicles makes a symmetric synapse onto a thick proximal dendrite 10 μm from the soma. (B) Numerous SR boutons synapse onto HRP-labeled (D) and unlabeled (uD) dendrites. (C) SR bouton with round vesicles forms an asymmetric synapse with a labeled dendrite approximately 125 μm from the soma. (D) Longitudinally-sectioned labeled dendrite is postsynaptic to SR boutons. (E) LR bouton makes asymmetric synapses with two different segments of an HRP-labeled dendrite. Labeled dendrites in B, D and E are approximately 75 μm from the soma. Note dispersed vesicles and large size of LR terminal compared to SR boutons, and the presence of mitochondria in LR boutons. Scale bar in E applies to all panels.

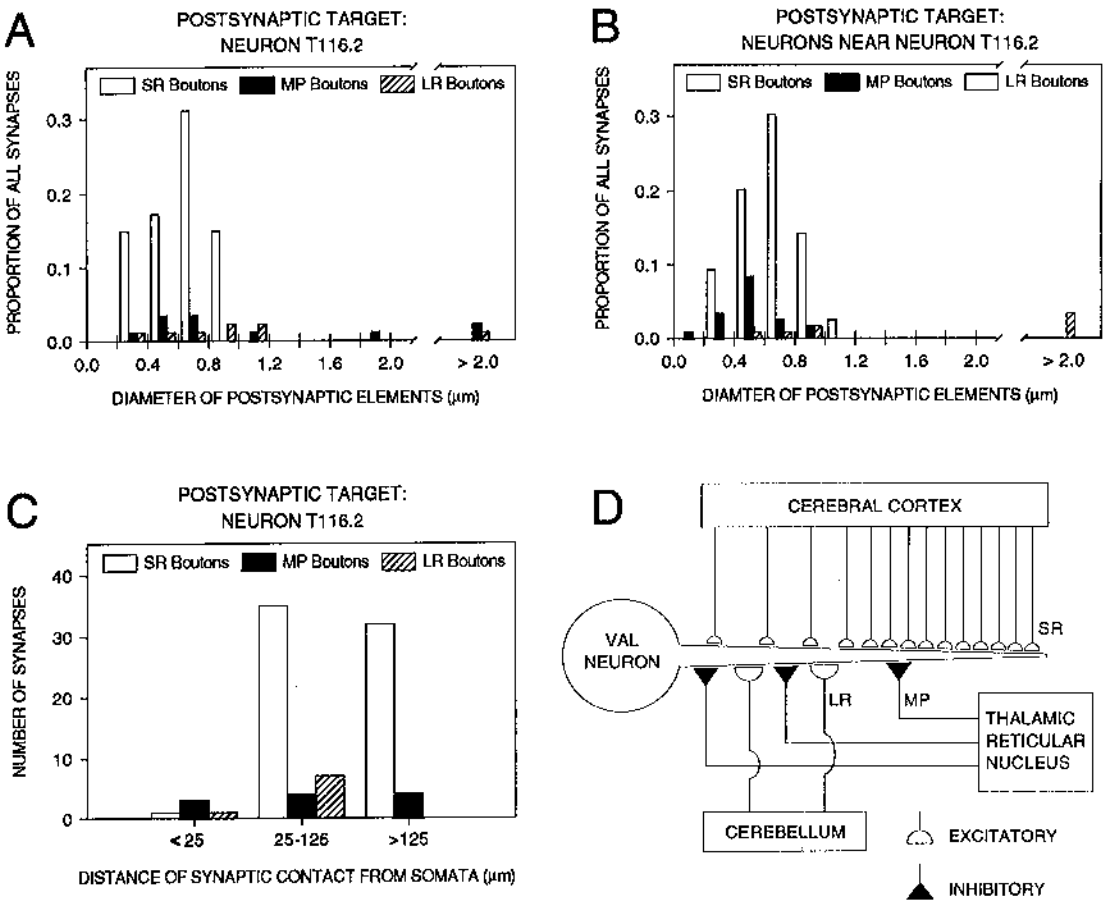

Fig. 11. Graphical and schematic representations of the synaptic organization of neurons in the VAL. (A, B) Histograms of the diameter of postsynaptic targets, for the HRP-labeled Type 3 (T116.2) neuron (A) and the surrounding unlabeled neuropil (B). The proportion of each of the three types of boutons that synapsed with a dendrite of a given cross-sectional diameter are displayed in bins of 0.2 μm increments. The "$>2.0\,\mu$m" bin corresponds to proximal dendrites and cell bodies. (C) Histogram of the sampling of distribution of bouton types along the length of the dendrite of neuron T116.2, revealing the density and spatial localization of afferents onto this neuron. (D) Schematic representation of the distribution and density of synaptic boutons onto neurons in the VAL, based on analysis of the intracellularly labeled neurons.

neurons in the surrounding neuropil (Fig. 11A, B; Kolmogorov–Smirnov test; $P < 0.05$).

DISCUSSION

Light microscopic anatomy of intracellularly labeled ventroanterior–ventrolateral neurons

Somatodendritic morphology. Intracellularly stained VAL neurons were classified as Type 1 ($N = 12$) or Type 3 ($N = 1$), classes previously recognized based on somatodendritic morphology using Golgi impregnation techniques.[92] Type 1 neurons resemble "tufted" or "multipolar bush" neurons typical of many thalamic nuclei, and this is the most commonly impregnated cell type with Golgi stains.[92] Both intracellularly- and Golgi-stained Type 1 cells have been found in all regions of the VAL. Taken together, these findings suggest that Type 1 neurons are the most prevalent morphological class of neurons in the VAL of rats. The other intracellularly labeled VAL neuron was located in rostral dorsolateral VAL and was distinguished by its large dendritic field, features characteristic of Golgi-impregnated Type 3 neurons. The absence of intracellularly stained Type 2 and Type 4 VAL neurons in this study was likely due to the presumed scarcity of these neuron types and the smaller sample of stained neurons in this study compared to the Golgi study. A previous intracellular labeling study of neurons in the VAL of rats depicted somatodendritic morphology similar to that described in the present report.[118] At present, no electrophysiological distinctions can be made between the morphologically-defined cell types in VAL (also see Refs 28 and 118).

Axon collaterals of ventroanterior–ventrolateral neurons in the thalamic reticular nucleus. Collaterals of thalamocortical axons provide an anatomical substrate for feedback inhibition of thalamic projection

neurons by GABAergic neurons in the TRN. Axon collaterals of intracellularly stained VAL neurons were not observed within dorsal thalamus, but all stained axons did give off one or more collaterals within the motor regions[13,100] of the TRN. These findings are in agreement with previous studies of collateralization patterns of thalamocortical neurons in a variety of thalamic nuclei,[28,38,48,95,108,120] although some investigators have reported that a small fraction of relay neurons emit collaterals in feline motor thalamus[119] and dorsal lateral geniculate nucleus (dLGN).[1,27,85,106] The absence of axon collaterals in dorsal thalamus refutes a critical anatomical premise of Andersen's model[2,3] of spindling genesis, in which rhythmic activity was proposed to emerge from the activation of thalamic inhibitory interneurons by recurrent axon collaterals of thalamocortical neurons.

VAL neurons exhibited different patterns of axon collateral arborization in the TRN, ranging from short, varicose, unbranched segments to long, varicose, richly branched collaterals. Although it cannot be ruled out that differences in collateralization patterns were due to incomplete staining, it is noteworthy that all main axons were heavily stained as they exited the TRN and many could be followed to the cortex. No relation was discerned between arborization patterns and either the somatodendritic morphology of VAL neurons or the location of the collaterals in the TRN. Similar conclusions have been drawn for functionally-characterized thalamic neurons in the ventrobasal nuclei of rats[38] and felines.[120] In contrast, collateral arborization patterns have been shown to differ between classes of functionally and anatomically distinguishable neurons in the dLGN.[27] A larger sampling of intracellularly stained VAL neurons will be needed to assess whether collateral arborization patterns are correlated with other anatomical and electrophysiological attributes.

Arbors of individual VAL axon collaterals were largely confined to narrow cylindrical fields oriented perpendicular to the parent axon, parallel to the borders of the TRN. Most neurons in the region of the TRN innervated by the VAL have long (200–600 μm) bipolar dendritic fields that also run parallel to the borders of the nucleus.[59,72,94,103,105] Therefore, since axon collaterals of VAL neurons run parallel to the orientation of TRN dendrites, individual VAL neurons are in a position to densely innervate a relatively small number of neurons in a relatively restricted slab of the TRN. Motor cortex and VAL project to overlapping regions of the TRN, and the motor cortical innervation of the TRN is arranged in a "lamellar" pattern that is restricted to parallel slabs of the TRN,[13] much like VAL axon collaterals. Thus, it is likely that motor-related, somatotopically-aligned cortical and thalamic inputs converge within the TRN as parallel slabs. Similar organizational arrangements are employed by other cortical–thalamic systems.[63] This suggests that the large elongated dendritic fields of TRN neurons provide a substrate for discrete, reciprocally-connected cortical and thalamic territories to map onto slabs of the TRN, rather than the more traditional view that the dendritic fields of TRN neurons introduce divergence into otherwise point-to-point cortical–thalamic connections.

Electron microscopic anatomy of intracellularly labeled ventroanterior–ventrolateral neurons

As described in this and an earlier study,[91] the fine structure of rat VAL is relatively simple compared to functionally-related nuclei in higher order mammals, owing to the absence of features characteristic of thalamic interneurons, such as vesicle-containing postsynaptic elements, dendrodendritic synapses and triadic synaptic arrangements. The neuronal cell bodies in the VAL have a homogeneous form that is typical of thalamic projection neurons. As mentioned above, these findings are consistent with the dearth of GABAergic neurons in the VAL of rats.[67,74,91]

Three classes of synaptic boutons were recognized in the VAL. SR boutons were the most common, and made asymmetric synapses primarily on distal dendrites. The distal location of SR boutons is consistent with the difficulty in reversing the cortically evoked EPSP with intrasomatic current injection.[93] In addition, the slow rise time of cortically evoked EPSPs[93] is likely related to the distal termination of these synapses (as well as spatial and temporal summation of these numerous inputs). A substantial proportion of the SR boutons in the VAL likely originates from the cerebral cortex,[55,115] much as in functionally-related nuclei in cats[32,52] and primates.[35]

LR boutons made multiple asymmetric synapses with intermediate and proximal dendrites. Many of these boutons undoubtedly originate from the cerebellar nuclei.[7,35,52,53,56,87] Recent reports also indicate that a small portion of corticothalamic boutons are similar to LR boutons in size, form and mode of synaptic contact.[39,96] Light microscopic studies of projections from motor cortex to thalamus in rats have revealed a mixture of small and large boutons in the posterior nucleus, but the innervation of the VAL consists exclusively of small boutons *terminaux* and *en passant*,[88] suggesting that few LR boutons in rat VAL are from cerebral cortex. Stimulation of cerebellar nuclei evokes EPSPs in VAL neurons that have a faster rise time than EPSPs evoked from cortical stimulation,[93] consistent with the more proximal dendritic termination of cerebellar input.

MP boutons formed symmetric synapses along the entire length of relay neuron dendrites, including the cell body. The MP boutons described in this study had a mode and site of termination and a morphology that were similar to GABAergic profiles previously identified in rat VAL,[91] and resemble "F" boutons[32] and glutamate decarboxylase-immunoreactive boutons[54] described in the ventroanterior and ventrolateral nuclei of feline thalamus. Many "F" boutons in rat ventrobasal complex and dLGN

are immunoreactive for subunits of $GABA_A$ receptors,[102,104] providing additional indirect evidence that MP boutons in the VAL are GABAergic. There are three possible sources of the MP boutons observed in the VAL: (i) interneurons, which, as mentioned above, are extremely scarce in the VAL of rats and are therefore unlikely to constitute a significant contributor; (ii) the entopeduncular nucleus and substantia nigra pars reticulata, which project to the ventromedial thalamic nucleus and portions of the VAL,[12,23,29,31] but not to the regions examined at the ultrastructural level in this study; and (iii) the TRN, which provides a GABAergic innervation of the VAL[13,19,42,91] and is likely to be the primary source of MP boutons in the tissue examined in this study. Consistent with this conclusion is the similarity in the morphology and synaptology of MP boutons and terminals originating from the TRN within a variety of nuclei in dorsal thalamus.[18,64,66,69,71,73,80]

In summary, the major features of the synaptic organization of thalamocortical neurons in rat VAL are: (i) a lower density of synapses on the soma and proximal dendrites than on intermediate and distal dendrites; (ii) boutons from cerebral cortex are prevalent, and synapse predominantly on distal dendrites; (iii) cerebellar inputs synapse on proximal dendrites; and (iv) inputs from the TRN synapse on proximal, intermediate and distal dendrites. This synaptic organization of thalamocortical neurons in rat VAL, as well as the morphological features of the presynaptic boutons, is similar to that described for corresponding nuclei in felines[50,51,53,54,56] and primates,[35,43,52,121] with the major distinction being the virtual absence of interneuronal synaptic circuitry in rat VAL.

Finally, cholinergic and non-cholinergic neurons in the laterodorsal tegmental nucleus, the pedunculopontine nucleus and other pontine and medullar reticular nuclei send widespread projections to dorsal thalamus in the rat.[10,11,21,33,62,81,82,90,98,101,117] Cholinergic boutons form symmetric and/or asymmetric synapses in different thalamic nuclei of mammals.[6,17,20,34,57,84,97,111] However, the innervation of VAL by these nuclei is apparently sparse, as indicated by anterograde transport studies[14,90] and the low levels of choline acetyltransferase immunolabeling in the VAL.[41,58] Likewise, monoaminergic neurons in the locus coeruleus,[21,22,30,70] dorsal raphe[21,30,70,78,112] and hypothalamus[75] project to dorsal thalamus, but sparsely to VAL in rats. Thus, these ascending projections are not likely to constitute a substantial contributor to the synaptic neuropil in the VAL.

Functional considerations

As revealed with intracellular recordings, the electrophysiological response properties and modes of firing (tonic vs rhythmic) of neurons in motor thalamus appear to be qualitatively similar in rats and cats,[93] in spite of the substantial differences in the extent of interneuronal circuitry in these nuclei. Analogous findings were obtained for recordings in the ventrobasal complex of rats (which has few interneurons) and higher order mammals (which have many interneurons).[5,37,79,89] These experimental results are consistent with compelling evidence that interneurons are not critical in setting the firing mode of relay neurons; this is apparently the domain of the TRN.[68,77,109,113] Left open, though, is the question of the functional role of thalamic interneurons, which apparently exert subtle effects on thalamic relay neurons that are not readily evident at a coarse level of analysis.

The vast majority of synapses made by interneurons consist of dendrodendritic synapses, with the GABAergic interneuronal dendrite as the presynaptic element. In thalamic nuclei possessing a substantial population of interneurons, triadic synaptic arrangements are common in which the excitatory subcortical afferent (e.g. cerebellum) synapses onto the dendrites of both relay neurons and interneurons, with the latter forming a GABAergic dendrodendritic synapse with the dendrite of the relay neuron.[47,50] As suggested by Ralston,[86] a depolarizing synaptic input onto dendrites of thalamic interneurons may evoke localized and graded dendritic neurotransmitter release in the absence of propagated spike activity. This circuitry is consistent with the disynaptic GABA-mediated feedforward inhibition observed in thalamic relay neurons following activation of excitatory subcortical afferents.[15,76] Since this early GABAergic inhibition in the thalamus entails an increase in membrane conductance to Cl^- ions via $GABA_A$ receptors,[15,110] the GABA released by interneuronal dendrites may produce a feedforward shunting of other synaptic influences onto relay neuron dendrites,[49,83] presumably within a localized domain along a dendrite. This, in essence, produces a spatially-localized voltage clamp. Taking into account that the dendritic membrane of relay neurons exhibits a variety of voltage- and Ca^{2+}-sensitive conductances and is probably excitable (e.g. high-threshold Ca^{2+} spikes),[45,46] thalamic relay neurons can be viewed conceptually as a collection of non-linear processors of afferent inputs (dendrites) that funnel into an axon spike generator (i.e. the cell body) that has two firing modes. Hence, thalamic interneurons can be considered to function primarily (i) in the realm of sculpting the duration and magnitude of afferent synaptic effects on the non-linear processing by relay neuron dendrites, and (ii) to affect the response properties of relay neuron dendrites, not by altering the firing pattern of relay neurons but rather in a localized fashion by modulating the electrotonic activation of dendritic voltage-sensitive conductances at restricted sites along dendrites.

Considering the above discussion, it is possible that the TRN has a dual role in the VAL of rats, in which cerebellar and cortical synaptic influences are "filtered" by different mechanisms. First, input from the cerebellar nuclei is potently excitatory, due in

part to the numerous synapses formed by individual cerebellothalamic axon terminals onto proximal dendrites of thalamic relay neurons. The transfer function of this input is largely dependent upon the operational firing mode of the thalamic relay neuron.[26,107] The TRN plays an important role in modulating the firing modes of relay neurons, thereby gating or filtering cerebellar inputs, i.e. a proximal-input filter. In this sense, the role of the TRN in thalamic function is similar in rats and higher order mammals. Second, synaptic activation of TRN input has the capacity to filter cortical input, but by different means. Excitatory axon terminals from the cerebral cortex terminate on distal dendrites of relay neurons, but even these inputs are capable of exerting an appreciable effect on the cell body due to the electrotonic compactness of thalamic neurons,[8,9,16] including rat VAL neurons.[93] As shown in this report, the majority of synapses onto relay neurons from MP boutons (presumed to correspond to boutons originating from the TRN) are positioned between the cell body and the distal cortical inputs. Hence, in the VAL of rats, the GABAergic input from the TRN has the capacity to shunt cortically-mediated synaptic currents in relay neuron dendrites, i.e. a distal-input filter. As discussed above, an analogous function may be the domain of interneurons in higher order mammals that have thalamic local circuit neurons, the major difference being that thalamic interneurons could perform such a function with a far greater degree of synaptic acuity.[24] For example, cortico-thalamic axons make synaptic contacts with both thalamocortical neurons and interneurons,[52,65,96,114] thereby providing a means for graded, subthreshold feedforward inhibition of thalamic projection neurons.

CONCLUSION

Hence, the development of interneuronal circuitry in motor-related thalamic nuclei of more phylogenetically advanced mammals (e.g. felines, primates) can be taken as an indication of a greater degree of synaptic integration and processing. Thalamic interneurons, which interact with relay neurons predominantly via dendritic release of GABA that is probably mediated in a graded, spike-independent manner, provide a substrate for spatially discrete, subthreshold inhibitory feedforward synaptic modulation. In contrast, in thalamic nuclei that have few or no interneurons, such as the VAL in rats, such modulatory mechanisms are restricted to spike-dependent input from the TRN that is driven by axon collaterals of corticothalamic and thalamocortical axons, i.e. a spatially diffuse, suprathreshold inhibitory feedforward and feedback synaptic interaction.

Acknowledgements—The authors thank Drs G. Buzsáki and B. Border for comments on the manuscript, and Elizabeth Harkins for assistance in histological staining of tissue. This study was supported by grants DA-02854 to P. M. G. and MH-45286 to J. M. T.

REFERENCES

1. Ahlsén G., Lindström S. and Sybirska E. (1978) Subcortical axon collaterals of principal cells in the lateral geniculate body of the cat. *Brain Res.* **156,** 106–109.
2. Andersen P. (1974) Physiological mechanism of barbiturate spindle activity. In *Basic Sleep Mechanisms* (eds Petre-Quadeus O. and Schlag J. D.), pp. 127–141. Academic Press, New York.
3. Andersen P. and Sears T. A. (1964) The role of inhibition in the phasing of spontaneous thalamo-cortical discharge. *J. Physiol., Lond.* **173,** 459–480.
4. Angaut P., Cicirata F. and Serapide F. (1985) Topographic organization of the cerebellothalamic projections in the rat. An autoradiographic study. *Neuroscience* **15,** 389–401.
5. Angel A. and Clarke K. A. (1975) An analysis of the representation of the forelimb in the ventrobasal complex of the albino rat. *J. Physiol., Lond.* **249,** 399–424.
6. Beaulieu C. and Cynader M. (1992) Preferential innervation of immunoreactive choline acetyltransferase synapses on relay cells of the cat's lateral geniculate nucleus: a double-labelling study. *Neuroscience* **47,** 33–44.
7. Bialowas J., Hassler R. and Wagner A. (1984) Types of synapses and degeneration in the thalamic nucleus ventralis oralis posterior after cerebellar lesions in the squirrel monkey. *J. Hirnforsch.* **25,** 417–437.
8. Bloomfield S. A., Hamos J. E. and Sherman S. M. (1987) Passive cable properties and morphological correlates of neurones in the lateral geniculate nucleus of the cat. *J. Physiol., Lond.* **383,** 653–692.
9. Bloomfield S. A. and Sherman S. M. (1989) Dendritic current flow in relay cells and interneurons of the cat's lateral geniculate nucleus. *Proc. natn. Acad. Sci. U.S.A.* **86,** 3911–3914.
10. Bolton R. F., Cornwall J. and Phillipson O. T. (1993) Collateral axons of cholinergic pontine neurones projecting to midline, mediodorsal and parafascicular thalamic nuclei in the rat. *J. chem. Neuroanat.* **6,** 101–114.
11. Carstens E., Leah J., Lechner J. and Zimmermann M. (1990) Demonstration of extensive brainstem projections to medial and lateral thalamus and hypothalamus in the rat. *Neuroscience* **35,** 609–626.
12. Carter D. A. and Fibiger H. C. (1978) The projections of the entopeduncular nucleus and globus pallidus in rat as demonstrated by autoradiography and horseradish peroxidase histochemistry. *J. comp. Neurol.* **177,** 113–123.
13. Cicirata F., Angaut P., Serapide M. F. and Panto M. R. (1990) Functional organization of the direct and indirect projection via the reticularis thalami nuclear complex from the motor cortex to the thalamic nucleus ventralis lateralis. *Expl Brain Res.* **79,** 325–337.
14. Cornwall J., Cooper J. D. and Phillipson O. T. (1990) Afferent and efferent connections of the laterodorsal tegmental nucleus in the rat. *Brain Res. Bull.* **25,** 271–284.
15. Crunelli V., Haby M., Jassik-Gerschenfeld D., Leresche N. and Pirchio M. (1988) Cl^-- and K^+-dependent inhibitory postsynaptic potentials evoked by interneurones of the rat lateral geniculate nucleus. *J. Physiol., Lond.* **399,** 153–176.

16. Crunelli V., Kelly J. S., Leresche N. and Pirchio M. (1987) The ventral and dorsal lateral geniculate nucleus of the rat: intracellular recordings *in vitro*. *J. Physiol., Lond.* **384,** 587–601.
17. Cucchiaro J. B., Uhlrich D. J. and Sherman S. M. (1988) Parabrachial innervation of the cat's dorsal lateral geniculate nucleus: an electron microscopic study using the tracer *Phaseolus vulgaris* leucoagglutinin (PHA-L). *J. Neurosci.* **8,** 4576–4588.
18. Cucchiaro J. B., Uhlrich D. J. and Sherman S. M. (1991) Electron-microscopic analysis of synaptic input from the perigeniculate nucleus to the A-laminae of the lateral geniculate nucleus in cats. *J. comp. Neurol.* **310,** 316–336.
19. de Biasi S., Frassoni C. and Spreafico R. (1986) GABA immunoreactivity in the thalamic reticular nucleus of the rat. A light and electron microscopical study. *Brain Res.* **399,** 143–147.
20. De Lima A. D., Montero V. M. and Singer W. (1985) The cholinergic innervation of the visual thalamus: an EM immunocytochemical study. *Expl Brain Res.* **59,** 206–212.
21. De Lima A. D. and Singer W. (1987) The brainstem projection to the lateral geniculate nucleus in the cat: identification of cholinergic and monoaminergic elements. *J. comp. Neurol.* **259,** 92–121.
22. Delagrange P., Conrath M., Geffard M., Tadjer D., Bouyer J. J. and Rougeul A. (1991) Noradrenaline-like terminals in the cat nucleus ventralis posterior of the thalamus. *Brain Res. Bull.* **26,** 533–537.
23. Deniau J. M., Kita H. and Kitai S. T. (1992) Patterns of termination of cerebellar and basal ganglia efferents in the rat thalamus. Strictly segregated and partly overlapping projections. *Neurosci. Lett.* **144,** 202–206.
24. Deschênes M. and Hu B. (1990) Electrophysiology and pharmacology of the corticothalamic input to lateral thalamic nuclei: an intracellular study in the cat. *Eur. J. Neurosci.* **2,** 140–152.
25. Donoghue J. P. and Parham C. (1983) Afferent connections of the lateral agranular field of the rat motor cortex. *J. comp. Neurol.* **217,** 390–404.
26. Filion M., LaMarre Y. and Cordeau J. P. (1971) Neuronal discharges of the ventrolateral nucleus of the thalamus during sleep and wakefulness in the cat. II. Evoked activity. *Expl Brain Res.* **12,** 499–508.
27. Friedlander M. J., Lin C. S., Stanford L. R. and Sherman S. M. (1981) Morphology of functionally identified neurons in lateral geniculate nucleus of the cat. *J. Neurophysiol.* **46,** 80–129.
28. Gazzara R. A., Fisher, Levine M. S., Hull C. D. and Buchwald N. A. (1986) Physiological and morphological analyses of ventral anterior and ventral lateral thalamic neurons in the cat. *Brain Res.* **397,** 225–237.
29. Gerfen C. R., Staines W. A., Arbuthnott G. W. and Fibiger H. C. (1982) Crossed connections of the substantia nigra in the rat. *J. comp. Neurol.* **207,** 283–303.
30. Groenewegen H. J. (1988) Organization of the afferent connections of the mediodorsal thalamic nucleus in the rat, related to the mediodorsal–prefrontal topography. *Neuroscience* **24,** 379–431.
31. Grofová I. (1989) Topographical organization of the nigrothalamic projections in the rat. *Soc. Neurosci. Abstr.* **15,** 1101.
32. Grofová I. and Rinvik E. (1974) Cortical and pallidal projections to the nucleus ventralis lateralis thalami. Electron microscopical studies in the cat. *Anat. Embryol.* **146,** 113–132.
33. Hallanger A. E., Levey A. I., Lee H. J., Rye D. B. and Wainer B. H. (1987) The origins of cholinergic and other subcortical afferents to the thalamus in the rat. *J. comp. Neurol.* **262,** 105–124.
34. Hallanger A. E., Price S. D., Lee H. J., Steininger T. L. and Wainer B. H. (1990) Ultrastructure of cholinergic synaptic terminals in the thalamic anteroventral, ventroposterior, and dorsal lateral geniculate nuclei of the rat. *J. comp. Neurol.* **299,** 482–492.
35. Harding B. N. and Powell T. P. S. (1977) An electron microscopic study of the centre-median and ventrolateral nuclei of the thalamus in the monkey. *Phil. Trans. R. Soc. Lond. Biol.* **279,** 357–412.
36. Haroian A. J., Massopust L. C. and Young P. A. (1981) Cerebellothalamic projections in the rat: an autoradiographic and degeneration study. *J. comp. Neurol.* **197,** 217–236.
37. Harris R. M. (1986) Morphology and physiologically identified thalamocortical relay neurons in the rat ventrobasal thalamus. *J. comp. Neurol.* **251,** 491–505.
38. Harris R. M. (1987) Axon collaterals in the thalamic reticular nucleus from thalamocortical neurons of the rat ventrobasal thalamus. *J. comp. Neurol.* **258,** 397–406.
39. Hoogland P. V., Wouterlood F. G., Welker E. and Van der Loos H. (1991) Ultrastructure of giant and small thalamic terminals of cortical origin: a study of the projections from the barrel cortex in mice using *Phaseolus vulgaris* leuco-agglutinin (PHA-L). *Expl Brain Res.* **87,** 159–172.
40. Horikawa K. and Armstrong W. E. (1988) A versatile means of intracellular labeling: injection of biocytin and its detection with avidin conjugates. *J. Neurosci. Meth.* **25,** 1–11.
41. Houser C. R., Phelps P. E. and Vaughn J. E. (1988) Cholinergic innervation of the rat thalamus as demonstrated by the immunocytochemical localization of choline acetyltransferase. In *Cellular Thalamic Mechanisms* (eds Bentivoglio M. and Spreafico R.), pp. 387–398. Elsevier Science, Amsterdam.
42. Houser C. R., Vaughn J. E., Barber R. P. and Roberts E. (1980) GABA neurons are the major cell type of the nucleus reticularis thalami. *Brain Res.* **200,** 341–354.
43. Ilinsky I. A. (1990) Structural and connectional diversity of the primate motor thalamus: experimental light and electron microscopic studies in the rhesus monkey. *Stereotactic Functional Neurosurg.* **54–55,** 114–124.
44. Itoh K., Konishi A., Nomura S., Mizuno N., Nakamura Y. and Sugimoto T. (1979) Application of coupled oxidation reaction to electron microscopic demonstration of horseradish peroxidase: cobalt–glucose oxidase method. *Brain Res.* **175,** 341–346.
45. Jahnsen H. and Llinás R. (1984) Electrophysiological properties of guinea-pig thalamic neurones: an *in vitro* study. *J. Physiol., Lond.* **349,** 205–226.
46. Jahnsen H. and Llinás R. (1984) Ionic basis for electroresponsiveness and oscillatory properties of guinea-pig thalamic neurones *in vitro*. *J. Physiol., Lond.* **349,** 227–247.
47. Jones E. G. (1985) *The Thalamus*. Plenum Press, New York.
48. Kita H. and Kitai S. T. (1986) Electrophysiology of rat thalamo-cortical relay neurons: an *in vivo* intracellular recording and labeling study. *Brain Res.* **371,** 80–89.
49. Koch C. (1985) Understanding the intrinsic circuitry of the cat's lateral geniculate nucleus: electrical properties of the spine–triad arrangement. *Proc. R. Soc. Lond. Ser. B* **225,** 365–380.

50. Kultas-Ilinsky K. and Ilinsky I. A. (1986) Neuronal and synaptic organization of the motor nuclei of mammalian thalamus. In *Currents Topics in Research on Synapses* (ed. Jones D. J.), pp. 77–145. Alan R. Liss, New York.
51. Kultas-Ilinsky K. and Ilinsky I. A. (1988) GABAergic systems of the feline motor thalamus: neurons, synapses and receptors. In *Cellular Thalamic Mechanisms* (eds Bentivoglio M. and Spreafico R.), pp. 349–363. Elsevier Science, Amsterdam.
52. Kultas-Ilinsky K. and Ilinsky I. A. (1991) Fine structure of the ventral lateral nucleus (VL) of the *Macaca mulatta* thalamus: cell types and synaptology. *J. comp. Neurol.* **314,** 319–349.
53. Kultas-Ilinsky K., Ilinsky I. A., Young P. A. and Smith K. R. (1980) Ultrastructure of degenerating cerebellothalamic terminals in the ventral medial nucleus of the cat. *Expl Brain Res.* **38,** 125–135.
54. Kultas-Ilinsky K., Ribak C. E., Peterson G. M. and Oertel W. H. (1985) A description of the GABAergic neurons and axon terminals in the motor nuclei of the cat thalamus. *J. Neurosci.* **5,** 1346–1369.
55. Kultas-Ilinsky K., Taylor J. and Smith K. R. (1976) Electron microscopy of corticothalamic degeneration in the rat. *Anat. Rec.* **184,** 454.
56. Kultas-Ilinsky K., Warton S., Tolbert D. L. and Ilinsky I. A. (1980) Quantitative and qualitative characteristics of dentate and fastigial afferents identified by electron microscopic autoradiography in the cat thalamus. *Brain Res.* **201,** 220–226.
57. Kuroda M. and Price J. L. (1991) Ultrastructure and synaptic organization of axon terminals from brainstem structures to the mediodorsal thalamic nucleus of the rat. *J. comp. Neurol.* **313,** 539–552.
58. Levey A. I., Hallanger A. E. and Wainer B. H. (1987) Choline acetyltransferase immunoreactivity in the rat thalamus. *J comp. Neurol.* **257,** 317–332.
59. Lübke J. (1993) Morphology of neurons in the thalamic reticular nucleus (TRN) of mammals as revealed by intracellular injections into fixed brain slices. *J. comp. Neurol.* **329,** 458–471.
60. McAllister J. P. and Wells J. (1981) The structural organization of the ventral posterolateral nucleus in the rat. *J. comp. Neurol.* **197,** 271–301.
61. McCormick D. A. (1992) Neurotransmitter actions in the thalamus and cerebral cortex and their role in neuromodulation of thalamocortical activity. *Prog. Neurobiol.* **39,** 337–388.
62. Mesulam M.-M., Mufson E. J., Wainer B. H. and Levey A. I. (1983) Central cholinergic pathways in the rat: an overview based on an alternative nomenclature (Ch1–Ch6). *Neuroscience* **10,** 1185–1202.
63. Mitrofanis J. and Guillery R. W. (1993) New views of the thalamic reticular nucleus in the adult and the developing brain. *Trends Neurosci.* **16,** 240–245.
64. Montero V. M. (1983) Ultrastructural identification of axon terminals from the thalamic reticular nucleus in the medial geniculate body in the rat: an EM autoradiographic study. *Expl Brain Res.* **51,** 338–342.
65. Montero V. M. (1991) A quantitative study of synaptic contacts on interneurons and relay cells of the cat lateral geniculate nucleus. *Expl Brain Res.* **86,** 257–270.
66. Montero V. M. and Scott G. L. (1981) Synaptic terminals in the dorsal lateral geniculate nucleus from neurons of the thalamic reticular nucleus: a light and electron microscope autoradiographic study. *Neuroscience* **6,** 2561–2577.
67. Mugnaini E. and Oertel W. H. (1985) An atlas of the distribution of GABAergic neurons and terminals in the rat CNS as revealed by GAD immunohistochemistry. In *Handbook of Chemical Neuroanatomy* (eds Björklund A. and Hökfelt T.), pp. 436–608. Elsevier Science, Amsterdam.
68. Mulle C., Steriade M. and Deschênes M. (1985) Absence of spindle oscillations in the cat anterior thalamic nuclei. *Brain Res.* **334,** 169–171.
69. Norita M. and Katoh Y. (1987) The GABAergic neurons and axon terminals in the lateralis medialis–suprageniculate nuclear complex of the cat: GABA-immunocytochemical and WGA–HRP studies by light and electron microscopy. *J. comp. Neurol.* **263,** 54–67.
70. Nothias F., Onteniente B., Roudier F. and Peschanksi M. (1988) Immunocytochemical study of serotoninergic and noradrenergic innervation of the ventrobasal complex of the rat thalamus. *Neurosci. Lett.* **95,** 59–63.
71. Ohara P. T. (1988) Synaptic organization of the thalamic reticular nucleus. *J. Electron Microsc. Tech.* **10,** 283–292.
72. Ohara P. T. and Lieberman A. R. (1985) The thalamic reticular nucleus of the adult rat: experimental anatomical studies. *J. Neurocytol.* **14,** 365–411.
73. Ohara P. T., Sefton A. J. and Lieberman A. R. (1980) Mode of termination of afferents from the thalamic reticular nucleus in the dorsal lateral geniculate nucleus of the rat. *Brain Res.* **197,** 503–506.
74. Ottersen O. P. and Storm-Mathisen J. (1984) GABA-containing neurons in the thalamus and pretectum of the rodent. An immunocytochemical study. *Anat. Embryol.* **170,** 197–207.
75. Panula P., Pirvola U., Auvinen S. and Airaksinen M. S. (1989) Histamine-immunoreactive nerve fibers in the rat brain. *Neuroscience* **28,** 585–610.
76. Paré D., Curró Dossi R. and Steriade M. (1991) Three types of inhibitory postsynaptic potentials generated by interneurons in the anterior thalamic complex of cat. *J. Neurophysiol.* **66,** 1190–1204.
77. Paré D., Steriade M., Deschênes M. and Oakson G. (1987) Physiological characteristics of anterior thalamic nuclei, a group devoid of inputs from reticular thalamic nucleus. *J. Neurophysiol.* **57,** 1669–1685.
78. Pasik P., Pasik T. and Holstein G. R. (1988) Serotonin-immunoreactivity in the monkey lateral geniculate nucleus. *Expl Brain Res.* **69,** 662–666.
79. Peschanski M., Lee C. L. and Ralston H. J. III (1984) The structural organization of the ventrobasal complex of the rat as revealed by the analysis of physiologically characterized neurons injected intracellularly with horseradish peroxidase. *Brain Res.* **297,** 63–74.
80. Peschanski M., Ralston H. J. III and Roudier F. (1983) Reticularis thalami afferents to the ventrobasal complex of the rat thalamus: an electron microscope study. *Brain Res.* **270,** 325–329.
81. Petrovicky P. (1990) Thalamic afferents from the brain stem. An experimental study using retrograde single and double labelling with HRP and iron–dextran in the rat. I. Medial and lateral reticular formation. *J. Hirnforsch.* **31,** 359–374.
82. Petrovicky P., Kolesárová D. and Slavínská V. (1990) Thalamic afferents from the brain stem. An experimental study using retrograde single and double labelling with HRP and iron–dextran in the rat. II. Nucleus laterodorsalis and subnucleus compactus nuclei pedunculo-pontini. *J. Hirnforsch.* **31,** 375–383.
83. Qian N. and Sejnowski T. J. (1990) When is an inhibitory synapse effective? *Proc. natn. Acad. Sci. U.S.A.* **87,** 8145–8149.

84. Raczkowski D. and Fitzpatrick D. (1989) Organization of cholinergic synapses in the cat's dorsal lateral geniculate and perigeniculate nuclei. *J. comp. Neurol.* **288,** 676–690.
85. Raczkowski D. and Sherman S. M. (1985) Morphology and physiology of single neurons in the medial interlaminar nucleus of the cat's lateral geniculate nucleus. *J. Neurosci.* **5,** 2702–2718.
86. Ralston H. J. III (1971) Evidence for presynaptic dendrites and a proposal for their mechanism of action. *Nature* **230,** 585–587.
87. Rinvik E. and Grofová I. (1974) Cerebellar projections to the nuclei ventralis lateralis and ventralis anterior thalami. Experimental electron microscopical and light microscopical studies in the cat. *Anat. Embryol.* **146,** 95–111.
88. Rouiller E. M., Liang F. Y., Moret V. and Wiesendanger M. (1991) Patterns of corticothalamic terminations following injection of *Phaseolus vulgaris* leucoagglutinin (PHA-L) in the sensorimotor cortex of the rat. *Neurosci. Lett.* **125,** 93–97.
89. Salt T. E. (1989) Gamma-aminobytyric acid and afferent inhibition in the cat and rat ventrobasal thalamus. *Neuroscience* **28,** 17–26.
90. Satoh K. and Fibiger H. C. (1986) Cholinergic neurons of the laterodorsal tegmental nucleus: efferent and afferent connections. *J. comp. Neurol.* **253,** 277–302.
91. Sawyer S. F., Martone M. E. and Groves P. M. (1991) A GABA immunocytochemical study of rat motor thalamus: light and electron microscopic observations. *Neuroscience* **42,** 103–124.
92. Sawyer S. F., Young S. J. and Groves P. M. (1989) Quantitative Golgi study of anatomically identified subdivisions of motor thalamus in the rat. *J. comp. Neurol.* **286,** 1–27.
93. Sawyer S. F., Young S. J., Groves P. M. and Tepper J. M. (1994) Cerebellar-responsive neurons in the thalamic ventroanterior–ventrolateral complex of rats: *in vivo* electrophysiology. *Neuroscience* **63,** 711–724.
94. Scheibel M. E. and Scheibel A. B. (1966) The organization of the nucleus reticularis thalami: a Golgi study. *Brain Res.* **1,** 43–62.
95. Scheibel M. E. and Scheibel A. B. (1966) The organization of the ventral anterior nucleus of the thalamus. A Golgi study. *Brain Res.* **1,** 250–268.
96. Schwartz M. L., Dekker J. J. and Goldman-Rakic P. S. (1991) Dual mode of corticothalamic synaptic termination in the mediodorsal nucleus of the rhesus monkey. *J. comp. Neurol.* **309,** 289–304.
97. Schwartz M. L. and Mrzljak L. (1993) Cholinergic innervation of the mediodorsal thalamic nucleus in the monkey: ultrastructural evidence supportive of functional diversity. *J. comp. Neurol.* **327,** 48–62.
98. Semba K., Reiner P. B. and Fibiger H. C. (1990) Single cholinergic mesopontine tegmental neurons project to both the pontine reticular formation and the thalamus in the rat. *Neuroscience* **38,** 643–654.
99. Sherman S. M. and Koch C. (1986) The control of retinogeniculate transmission in the mammalian lateral geniculate nucleus. *Expl Brain Res.* **63,** 1–20.
100. Shosaku A., Kayama Y., Sumitomo I., Sugitani M. and Iwama K. (1989) Analysis of recurrent inhibitory circuit in rat thalamus: neurophysiology of the thalamic reticular nucleus. *Prog. Neurobiol.* **32,** 77–102.
101. Sofroniew M. V., Priestley J. V., Consolazione A., Eckenstein F. and Cuello A. C. (1985) Cholinergic projections from the midbrain and pons to the thalamus in the rat, identified by combined retrograde tracing and choline acetyltransferase immunohistochemistry. *Brain Res.* **329,** 213–223.
102. Soltesz I., Roberts J. D. B., Takagi H., Richards J. G., Mohler H. and Somogyi P. (1990) Synaptic and nonsynaptic localization of benzodiazepine/$GABA_A$ receptor Cl^- channel complex using monoclonal antibodies in the dorsal lateral geniculate nucleus of the cat. *Eur. J. Neurosci.* **2,** 414–429.
103. Spreafico R., Battaglia G. and Frassoni C. (1991) The reticular thalamic nucleus (RTN) of the rat: cytoarchitectural, Golgi, immunocytochemical, and horseradish peroxidase study. *J. comp. Neurol.* **304,** 478–490.
104. Spreafico R., de Biasi S., Amadeo A. and de Blas A. L. (1993) $GABA_A$-receptor immunoreactivity in the rat dorsal thalamus: an ultrastructural investigation. *Neurosci. Lett.* **158,** 232–236.
105. Spreafico R., de Curtis M., Frassoni C. and Avanzini G. (1988) Electrophysiological characteristics of morphologically identified reticular thalamic neurons from rat slices. *Neuroscience* **27,** 629–638.
106. Stanford L. R., Friedlander M. J. and Sherman S. M. (1983) Morphological and physiological properties of geniculate W-cells of the cat: a comparison with X- and Y-cells. *J. Neurophysiol.* **50,** 582–608.
107. Steriade M., Apostol V. and Oakson G. (1971) Control of unitary activities in cerebellothalamic pathway during wakefulness and synchronized sleep. *J. Neurophysiol.* **34,** 389–413.
108. Steriade M. and Deschênes M. (1984) The thalamus as a neuronal oscillator. *Brain Res. Rev.* **8,** 1–63.
109. Steriade M., Deschênes M., Domich L. and Mulle C. (1985) Abolition of spindle oscillations in thalamic neurons disconnected from nucleus reticularis thalami. *J. Neurophysiol.* **54,** 1473–1497.
110. Steriade M. and Llinás R. (1988) The functional states of the thalamus and the associated neuronal interplay. *Physiol. Rev.* **68,** 649–742.
111. Uhlrich D. J., Cucchiaro J. B. and Sherman S. M. (1988) The projection of individual axons from the parabrachial region of the brain stem to the dorsal lateral geniculate nucleus in the cat. *J. Neurosci.* **8,** 4565–4575.
112. Vertes R. P. (1991) A PHA-L analysis of ascending projections of the dorsal raphe nucleus in the rat. *J. comp. Neurol.* **313,** 643–668.
113. von Krosigk M., Bal T. and McCormick D. A. (1993) Cellular mechanism of a synchronized oscillation in the thalamus. *Science* **261,** 361–364.
114. Weber A. J., Kalil R. E. and Behan M. (1989) Synaptic connections between corticogeniculate axons and interneurons in the dorsal lateral geniculate nucleus of the cat. *J. comp. Neurol.* **289,** 156–164.
115. Williams M. N. and Faull R. L. M. (1987) The distribution and morphology of identified thalamocortical projection neurons and glial cells with reference to the question of interneurons in the ventrolateral nucleus of the rat thalamus. *Neuroscience* **21,** 767–780.
116. Wilson C. J. and Groves P. M. (1979) A simple and rapid section embedding technique for sequential light and electron microscopic examination of individually stained central neurons. *J. Neurosci. Meth.* **1,** 383–391.
117. Woolf N. J. and Butcher L. L. (1986) Cholinergic systems in the rat brain: III. Projections from the ponto-mesencephalic tegmentum to the thalamus, tectum, basal ganglia, and basal forebrain. *Brain Res. Bull.* **16,** 603–637.
118. Yamamoto T., Kishimoto Y., Yoshikawa H. and Oka H. (1991) Intracellular recordings from rat thalamic VL neurons: a study combined with intracellular staining. *Expl Brain Res.* **87,** 245–253.

119. Yamamoto T., Noda T., Samejima A. and Oka H. (1985) A morphological investigation of thalamic neurons by intracellular HRP staining in cats. *J. comp. Neurol.* **236,** 331–347.
120. Yen C.-T, Conley M. and Jones E. G. (1985) Morphological and functional types of neurons in cat ventral posterior thalamic nucleus. *J. Neurosci.* **5,** 1316–1338.
121. Yi H., Ilinsky I. A. and Kultas-Ilinsky K. (1993) Reticular thalamic nucleus input to the nuclei of the monkey thalamus: light and electron microscopic study. *Soc. Neurosci. Abstr.* **19,** 1436.
122. Young S. J., Royer S. M., Groves P. M. and Kinnamon J. C. (1987) Three-dimensional reconstructions from serial micrographs using the IBM PC. *J. Electron Microsc. Tech.* **6,** 207–217.

(*Accepted* 7 *June* 1994)